THE GEOLOGICAL SOCIETY OF AMERICA®

Finding the Mean and 95 Percent Confidence Interval of a Set of Strike-and-Dip or Lineation Data

VINCENT S. CRONIN

Department of Geology, Baylor University, One Bear Place #97354, Waco, TX 76798-7354

Key Terms: ***Field Methods, Uncertainty, Fisher Statistics, Spherical Data***

ABSTRACT

Quantitative observational data should be reported with appropriate uncertainty estimates. Statistical methods developed by Fisher (1953) to analyze paleomagnetic data are also useful for determining the 95 percent confidence interval associated with site mean strike and dip from three or more observations (at least seven observations preferred) of the orientation of geologic surfaces that are approximately homoclinal or of lineations that are subparallel. The uncertainty in the strike of a surface is a function of the uncertainty and inclination of the dip vector and is greater than the dip uncertainty. For example, surfaces with measured orientations (strike and dip) of 310° 38°NE, 319° 45°NE, and 322° 30°NE at a given site have a site mean orientation of 317 ± 18° and 38 ± 14°NE at a 95 percent confidence interval.

INTRODUCTION

The assessment, quantification, and minimization of error are of central importance in science. It may be asserted that a quantitative measurement stated without an error estimate is not a scientific observation.

One basic geological task in which the quantification of observational variability is commonly neglected is measuring the orientation of lineations or the strike and dip of bedding, faults, or joints at a given site. These data are essential to many projects undertaken by geologists, such as basic field mapping, slope stability analysis, projection of geologic features onto cross sections and fault-plane maps, and development of models of subsurface geology. If it is important to accurately measure and report the orientation of geological surfaces or lineations at a site, it should be important to compute and report the uncertainty of those data as well.

Student geologists have been encouraged to measure several attitudes and to informally average them to define the mean orientation that is characteristic of the site. In practice, this averaging may involve a variety of more-or-less *ad hoc* strategies, including (1) informally estimating an average strike azimuth and an average dip angle by eye, (2) graphically estimating a mean value from stereonet plots of poles to planes, and (3) computing average dip vectors or vector normals by unit-vector addition. Obtaining a mean orientation by summing unit vectors is a defensible strategy, but that mean orientation does not by itself contain important information about the variability of the input data.

Paleomagnetic workers confronted this same problem in a slightly different form decades ago (e.g., Fisher, 1953; Irving, 1964; and Tarling, 1971). These workers typically have three or more samples taken from a given site, each characterized by a magnetic declination (comparable to a lineation trend or a surface dip azimuth) and inclination (comparable to a plunge or dip angle). From these data, a site mean magnetic vector orientation is obtained along with an estimate of the precision of these observations.

The goals of this article are (1) to describe the use of Fisher's (1953) statistical method for assessing the mean orientation of a set of vectors, the radius of the 95 percent confidence interval (CI) cone around that mean unit vector, and the estimated value of the precision or concentration parameter, k, used to give an assessment of the colinearity of the vectors; (2) to introduce the corresponding estimate of strike uncertainty; and (3) to facilitate the use of this method by practicing geologists by presenting a worked example and by making available spreadsheet code that implements Fisher's statistics to determine a mean orientation and 95 percent CI for a set of 3–12 lineations or surface orientations at a given site. The spreadsheet is accessible online through the journal website. A more complete development of statistical theory is beyond the scope of this article and is available elsewhere (e.g., Fisher, 1953; Irving, 1964; Mardia, 1972; Batschelet, 1981; Fisher et al., 1987; Opdyke and Channell, 1996; Tauxe, 1998; and Borradaile, 2003). The explanations offered in this paper are directed toward the practicing geologist or student who may not be familiar with the statistical

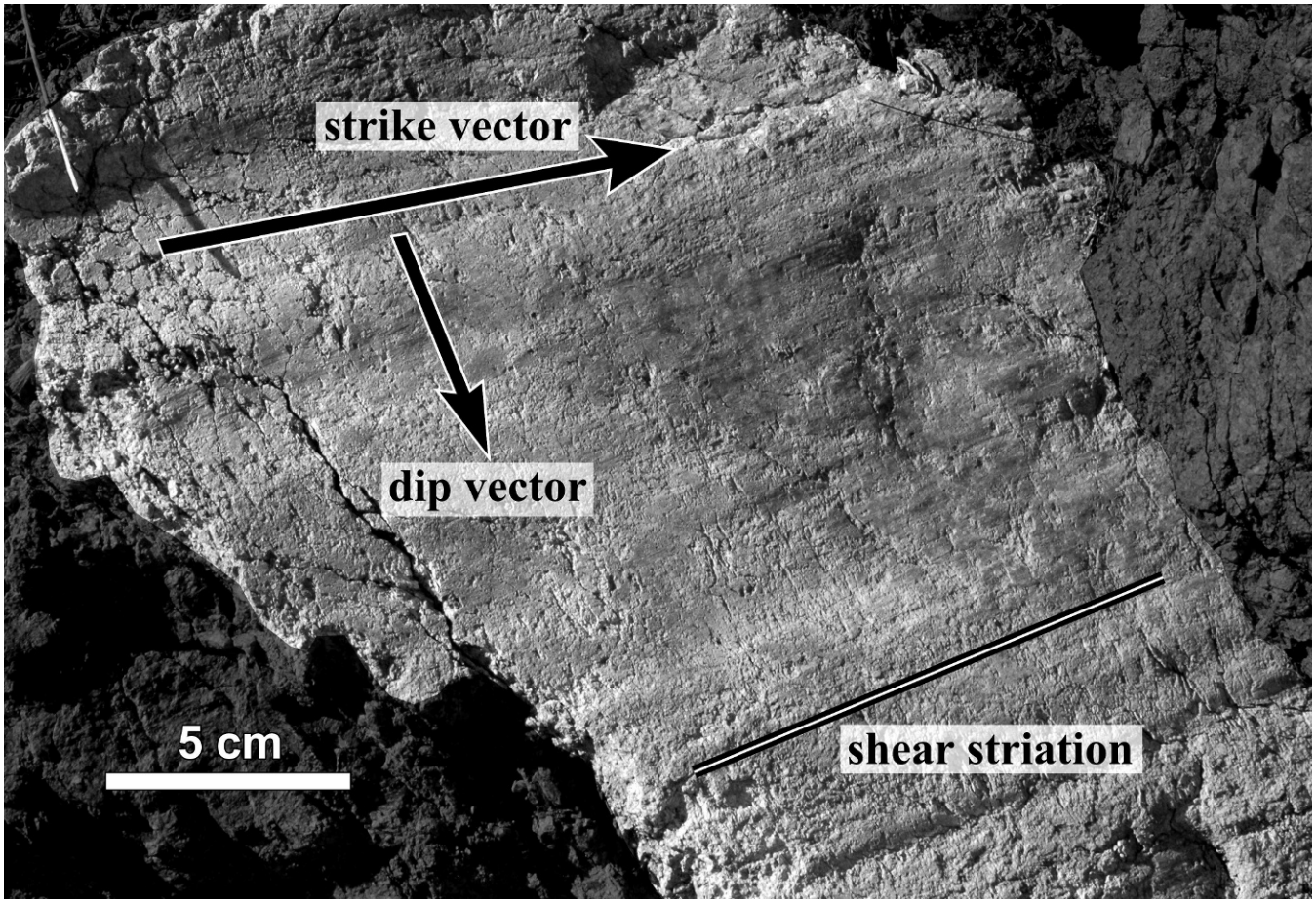

Figure 1. Photograph illustrating the principal question addressed in this article: How does a geoscientist determine the average orientation and associated uncertainty of a geological surface or a set of lineations? Fault surface with shear striations from the central Santa Monica Mountains near Malibu, southern California. The direction of the strike vector (i.e., the reference strike direction) is specified using the right-hand–rule convention.

treatment of the type of orientation data that we commonly collect at outcrops and in trenches, boreholes, and cores containing near-parallel lineations or surfaces.

It is important to recognize that this statistical method is intended for unimodal orientation data: orientations that approximate a normal distribution around a single mean direction (i.e., a *Fisher distribution*; see Fisher et al., 1987). For example, this method is appropriate for defining the mean and 95 percent CI uncertainty for several observations of the orientation of lineations or surfaces that are locally subparallel to one another within the same structural domain. Examples include the mean orientation of several adjacent points on the same geologic surface (e.g., a bedding, fault, or joint surface), the mean orientation of multiple subparallel beds, or the mean orientation of shear lineations on a fault surface (Figure 1). This method would not be appropriate for characterizing the varied orientations of beds on different limbs of a fold.

METHOD

The format in which the raw field data are recorded tends to vary among different workers. Geologists record orientation data for planar features in the field using one of several different conventions (e.g., quadrant, azimuth, right-hand rule, dip direction). The orientation of a lineation may be recorded in terms of a rake or pitch on a specified plane or as plunge and trend directly if a strata compass is used. Regardless of the method used to record the data in the field, it is simplest to convert each set of orientation data to plunge angle and trend azimuth so that they can be more easily manipulated by computer code. In this article, surface-orientation data are presented as the plunge and trend of the dip vector. By convention among geologists, a downward-directed plunge is a positive-signed angle. This is compatible with the similar convention used in paleomagnetic analysis, in which a downward-directed inclination is a positive-signed angle (e.g., Tauxe, 1998).

In general practice, directional or angular data collected in the field are expressed in degrees of arc. Noting that the default condition in many spreadsheets and programming languages is to operate on angles expressed in radian measure, all angles referenced in this article will be in degrees for the sake of clarity.

The direction cosines $\{l_i, m_i, n_i\}$ for each observation are determined relative to axes oriented north, east, and downward.

$$\begin{aligned} l_i &= \cos(p_i)\cos(t_i) \qquad m_i = \cos(p_i)\sin(t_i) \\ n_i &= \sin(p_i) \end{aligned} \tag{1}$$

where p_i and t_i are, respectively, the plunge and trend of the ith observation. The direction cosines for the mean dip vector $\{\bar{l}, \bar{m}, \bar{n}\}$ are found by summing the direction cosines for each axial direction.

$$\bar{l} = \sum_{i=1}^{N} l_i \qquad \bar{m} = \sum_{i=1}^{N} m_i \qquad \bar{n} = \sum_{i=1}^{N} n_i \tag{2}$$

The length of the mean dip vector is R, where

$$R = \sqrt{\bar{l}^2 + \bar{m}^2 + \bar{n}^2}. \tag{3}$$

The corresponding unit vector $\{\hat{l}, \hat{m}, \hat{n}\}$ is found by dividing each direction cosine of the mean dip vector by R.

$$\hat{l} = \frac{\bar{l}}{R} \qquad \hat{m} = \frac{\bar{m}}{R} \qquad \hat{n} = \frac{\bar{n}}{R} \tag{4}$$

The direction cosines are converted to the trend and plunge of the mean dip vector.

$$\delta = \arcsin(\hat{n}) \tag{5}$$

where δ is the plunge of the mean dip vector. If $\hat{m} \geq 0$,

$$\text{trend} = \left[\arccos\left(\frac{\hat{l}}{\cos(\arcsin(\hat{n}))}\right)\right] \tag{6a}$$

or if $\hat{m} < 0$,

$$\text{trend} = 360 - \left[\arccos\left(\frac{\hat{l}}{\cos(\arcsin(\hat{n}))}\right)\right]. \tag{6b}$$

Variable N is the number of observations. The estimated value of the precision parameter k ranges from 0 for a vector set that is strongly noncolinear to ∞ for vectors that are perfectly colinear, as when $N = R$:

$$k = (N - 1)/(N - R) \tag{7}$$

(Fisher, 1953; Tarling, 1971; and Opdyke and Channell, 1996). Paleomagnetic workers describe acceptably precise (class I) orientation data as having k values of 10 or greater, although Tarling (1971) notes that k may not be a reliable indicator of precision for $N < 7$, suggesting that seven or more observations should be made at a site to reliably classify the site-data quality.

The angular radius of the 95 percent CI cone (α_{95}) is

$$\alpha_{95} = \arccos\left(1 - \left\{\left(\frac{N - R}{R}\right)\left[\left(\frac{1}{P}\right)^{1/(N-1)} - 1\right]\right\}\right) \tag{8}$$

where probability $P = 0.05$ (e.g., Fisher, 1953; Tauxe, 1998). This indicates that we are 95 percent confident that the mean vector for a hypothetical large population of measurements would be located within a cone of radius α_{95} degrees from the mean vector of our much more limited sample. In other words, there is only a 1-in-20 chance that the mean vector of that hypothetical large population of observations lies outside of a cone of radius α_{95} degrees from our sample mean vector.

The analysis presented to this point assesses the variability of the input orientation data independent of any consideration of possible random errors in measurement, such as the 0.5° to 1° error commonly estimated for the Brunton compass (e.g., Compton, 1962; Brunton Company, 2000). If it is desirable to account for this random measurement error, which is assumed to be uncorrelated with the error associated with the intrinsic variability of the measured quantity, the radius of the total error region (r_{total}) is given by

$$r_{\text{total}} = \sqrt{(\alpha_{95})^2 + M^2} \tag{9}$$

where variable M is the estimated random measurement error.

Derivation of Strike Uncertainty Expression

Fisher's statistical method defines the cone-shaped uncertainty region around the mean dip vector. However, the angular uncertainty in the orientation of a dip vector is not the same as the uncertainty in the strike direction. In the limit as the plunge of the dip vector approaches 0, the strike uncertainty and the dip uncertainty trend toward convergence; however, the strike is undefined when the dip is

horizontal. As the plunge of the mean dip vector increases, the uncertainty in the trend of the dip vector increases, with a corresponding increase in strike uncertainty, given that strike is $\pm 90^\circ$ from the dip trend. The strike uncertainty is always greater than the dip uncertainty and is a function of the dip angle and the dip uncertainty.

An expression that relates the strike uncertainty (β) to the mean dip angle (δ) and the angular radius of the uncertainty region (r_{total}) can be derived as follows. Consider a cone with sides of unit length and angular radius r_{total}, coinciding with the apex of the uncertainty region around the dip vector (Figure 2a). The radius of the circle at the base of the cone is $\sin(r_{total})$, and the distance from the apex of the cone to the center of its base along the mean dip vector is $\cos(r_{total})$. The point at the apex of the cone is labeled A, and the point at the center of the cone's base is labeled B.

For a mean dip vector inclined at angle δ from horizontal, the length of the horizontal segment from point A to the point directly above point B (point B′ in Figure 2b) is $[\cos(r_{total})\cos(\delta)]$. The projection of the base of the cone onto a horizontal plane (Figure 2c) is an ellipse for all angles δ in the range $[0 < \delta < 90^\circ]$, and the projection of the sides of the cone are line segments that are tangent to that ellipse and that pass through point A. The length of the semiminor axis of the ellipse (i.e., the shortest distance from B' to the ellipse) is $[\sin(r_{total})\sin(\delta)]$, and the semimajor axis length is $\sin(r_{total})$.

Group points A and B', the ellipse, and the two lines tangent to the ellipse through A together into a set of geometric objects. Then homogeneously shorten the set by the ratio of the semiminor to the semimajor axes (i.e., by $[\sin(r_{total})\sin(\delta)]/\sin(r_{total})$) in a direction parallel to the major axis of the ellipse. The result will be a circle centered on point B' and two lines tangent to the circle through point A (Figure 2d). The circle has a radius of $[\sin(r_{total})\sin(\delta)]$, identical to the semiminor axis of the ellipse. The distance between A and B' is unchanged.

Label the tangent point C, and recall from elementary geometry that segment AC is perpendicular to CB' (Figure 2d). Define point D along segment AB' by constructing right triangle CDB'. Angle DCB' is equal to angle CAB' and is labeled θ. Points C, A, and B' form a right triangle in which the length of line segment CB' is $[\sin(r_{total})\sin(\delta)]$ (i.e., the radius of the circle) and the length of line segment AB' is $[\cos(r_{total})\cos(\delta)]$, so angle θ is given by

$$\theta = \arcsin\left(\frac{\sin(r_{total})\sin(\delta)}{\cos(r_{total})\cos(\delta)}\right). \qquad (10)$$

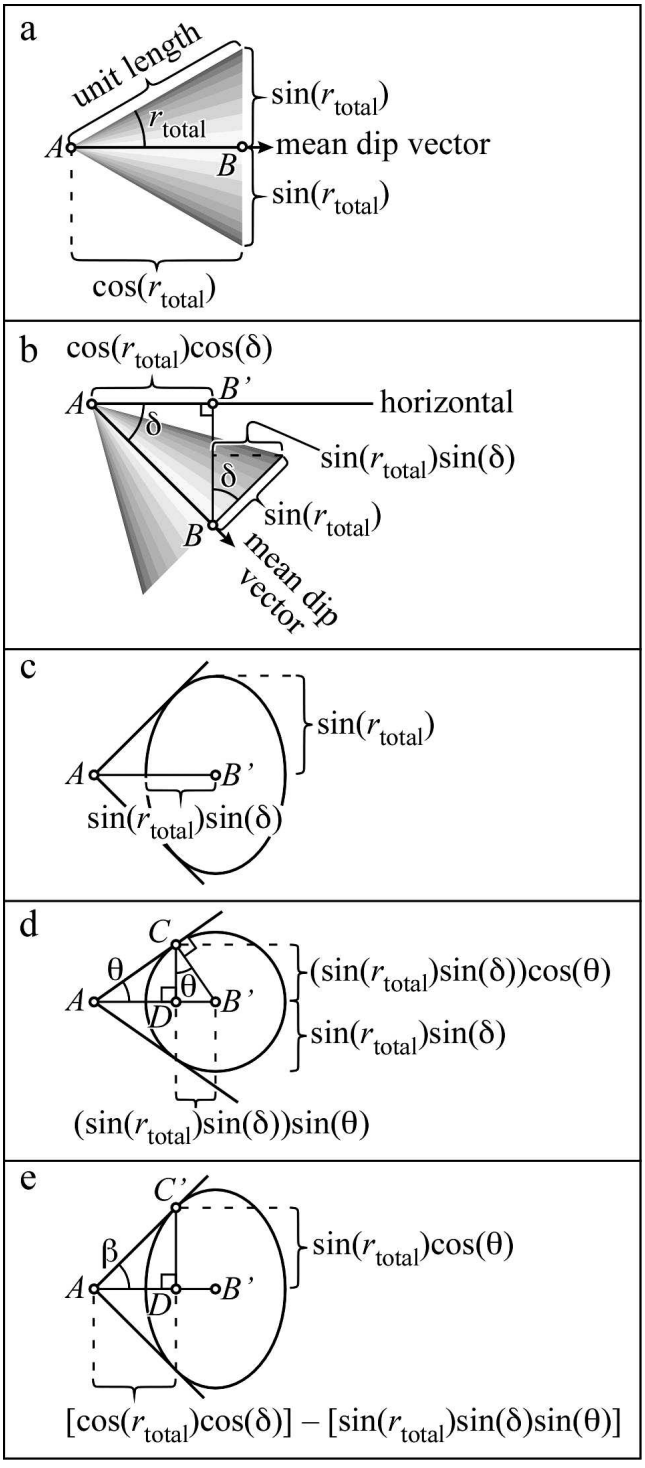

Figure 2. Derivation of strike uncertainty. See text for explanation.

The length of line segment CD is $[(\sin(r_{total})\sin(\delta))\cos(\theta)]$, noting that points C, D, and B' form a right triangle. We now take the set of grouped objects and homogeneously stretch them by the ratio of the semimajor to the semiminor axes (i.e., by $\sin(r_{total})$/

[$\sin(r_{\text{total}})\ \sin(\delta)$]) in a direction parallel to the major axis of the ellipse, thereby restoring the original configuration (Figure 2e). For clarity, we relabel the tangent point C' and define the length of segment DC' by noting that segment DC has been stretched parallel to itself by the same ratio as all other objects:

$$\text{segment length } DC' = \sin(r_{\text{total}})\sin(\delta)\cos(\theta)\left(\frac{\sin(r_{\text{total}})}{\sin(r_{\text{total}})\sin(\delta)}\right) \quad (11)$$

which simplifies to [$\sin(r_{\text{total}})\ \cos(\theta)$]. Angle $C'AB'$ is labeled β and is the angle between the trend of the mean dip vector and the strike of the vertical plane that is tangent to the uncertainty cone around the mean dip vector. Consequently, angle β is the uncertainty in strike direction. Considering right triangle $C'AB'$, the strike uncertainty (β) is given by

$$\beta = \arctan\left(\frac{\sin(r_{\text{total}})\cos(\theta)}{(\cos(r_{\text{total}})\cos(\delta)) - (\sin(r_{\text{total}})\sin(\theta)\sin(\delta))}\right). \quad (12)$$

Eq. 12 defines the angular uncertainty in strike (β) as a function of the dip-vector uncertainty (r_{total}) and the plunge of the mean dip vector (δ) and is valid in the range [$0 < \delta < (90^\circ - r_{\text{total}})$]. Strike is undefined for any plane whose dip vector is horizontal. In the limit as the value of δ approaches ($90^\circ - r_{\text{total}}$), the strike uncertainty approaches $\pm 90^\circ$. When $\delta > (90^\circ - r_{\text{total}})$, all strike directions are admissible.

WORKED EXAMPLE

One of the goals of this article is to facilitate the use of Fisher statistics by practicing geologists. A reasonable strategy toward achieving that goal is to examine a worked example of the method. The numerical values given in intermediate steps throughout the example below are rounded to four decimal places, just as they might be displayed in a spreadsheet. In practice, intermediate values are not rounded but are carried through to the end of the process, and the results are expressed to the same number of significant figures as the input data: integer degrees in, integer degrees out.

At least seven observations of the orientation of a surface or lineation should be made; however, for the sake of economy, the following example uses just three orientation measurements to illustrate the method. The observations of the strike and dip of a surface are 310° 38°NE, 319° 45°NE, and 322° 30°NE. The dip-vector trend is 90° from strike, with a plunge equal to the dip angle (e.g., trend azimuth is 40° and plunge is 38° for the plane 310° 38°NE).

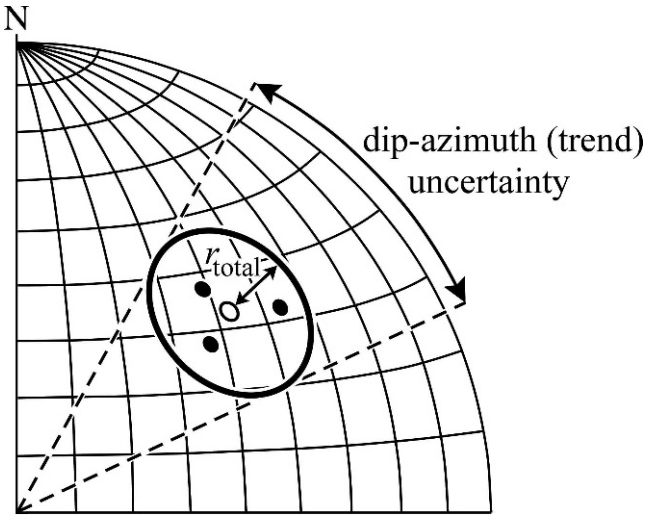

Figure 3. Northeast quadrant of lower-hemisphere Lambert equal-area projection, showing the three dip vectors in the example (black circles), the mean dip vector (white-filled circle), the 95 percent confidence interval around the mean (bold oval), and the associated uncertainty region for the dip azimuth (bounded by dashed lines).

	Strike and dip	Dip-vector plunge	Dip-vector trend
observation 1	310° 38°NE	38°	40°
observation 2	319° 45°NE	45°	49°
observation 3	322° 30°NE	30°	52°

The direction cosines are determined relative to north-, east-, and down-directed axes for each observation (Eq. 1).

	l_i	m_i	n_i
observation 1	0.6037	0.5065	0.6157
observation 2	0.4639	0.5337	0.7071
observation 3	0.5332	0.6824	0.5000

The direction cosines for the mean dip vector are found by summing the direction cosines for each axial direction (Eq. 2).

	$\bar{l}$	$\bar{m}$	$\bar{n}$
mean vector	1.6007	1.7226	1.8228

The length of the mean dip vector is

$$R = \sqrt{1.6007^2 + 1.7226^2 + 1.8228^2} \approx 2.9753$$

(Eq. 3). The components of the corresponding unit vector are

	$\hat{l}$	$\hat{m}$	$\hat{n}$
unit mean vector	0.5380	0.5790	0.6126

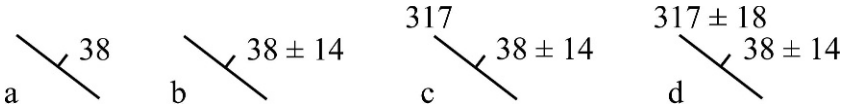

Figure 4. Map symbols for site mean strike and dip for given example. (a) Traditional map symbol. (b) Map symbol with 95 percent confidence interval (CI) for dip angle. (c) Preferred map symbol indicating 95 percent CI uncertainty for dip angle and explicitly noting reference strike azimuth (right-hand rule). (d) Map symbol with explicit notation of strike azimuth, dip angle, and their associated 95 percent CI uncertainties.

(Eq. 4). The direction cosines of the unit mean vector are converted to the plunge and trend of the mean dip vector (Eqs. 5 and 6a), given that $\hat{m} \geq 0$ in this example:

$$\delta = \arcsin(0.6126) \approx 38^\circ$$

so the plunge is 38°, and

$$\text{trend} = \left[\arccos\left(\frac{0.5380}{\cos(\arcsin(0.6126))}\right)\right] \approx 47^\circ.$$

The estimated value of the precision parameter $k = (3 - 1)/(3 - 2.9753) \approx 81$ (Eq. 7), so this is considered to be a class I data set; however, the small size of the data set casts some doubt on the reliability of that classification. Ideally, we should have at least seven observations. The angular radius of the 95 percent CI cone (Eq. 8) is

$$\alpha_{95} = \arccos\left(1 - \left\{\left(\frac{3 - 2.9753}{2.9753}\right)\left[\left(\frac{1}{0.05}\right)^{1/(3-1)} - 1\right]\right\}\right) \approx 14^\circ.$$

If a compass error of 1° is assumed, the radius of the total uncertainty region is changed by an insignificant amount:

$$r_{\text{total}} = \sqrt{14^2 + 1^2} \approx 14^\circ$$

(Eq. 9). The uncertainty in the dip azimuth, and hence in the strike azimuth, is

$$\text{strike uncertainty} = \pm \arctan\left(\frac{\sin(14^\circ)\cos(11^\circ)}{(\cos(14^\circ)\cos(38^\circ)) - (\sin(14^\circ)\sin(11^\circ)\sin(38^\circ))}\right) \approx 18^\circ$$

where

$$\theta = \arcsin\left(\frac{\sin(14^\circ)\sin(38^\circ)}{\cos(14^\circ)\cos(38^\circ)}\right) \approx 11^\circ$$

(Eqs. 10 and 12). The result is a mean surface orientation with a strike of 317 ± 18° and a dip angle of 38 ± 14°NE (Figure 3).

The site mean orientation data are usually represented on a map using a strike-and-dip symbol with the dip angle explicitly stated (Figure 4a). It might be better practice to include the 95 percent CI uncertainty as part of the map symbol. The most economical option would be to include the uncertainty in the dip angle explicitly, from which the strike uncertainty can be computed using Eqs. 10 and 12 (Figure 4b). My preferred symbol includes an explicit notation of the azimuth of the reference strike defined by the right-hand rule (Figure 4c), added to avoid measurement errors by users of the map. A variant of this would include the strike uncertainty as well (Figure 4d), which saves the user from making a calculation but adds an avoidable distraction to the map.

ACKNOWLEDGMENTS

Doug Burbank, Gary Johnson, and Noye Johnson introduced the author to Fisher statistics while at Dartmouth College. This paper was improved by comments by Sam Patterson at a workshop on quantitative methods, organized by Cathy Manduca and Heather Macdonald at the Science Education Resource Center at Carleton College. Helpful suggestions offered by Brian Bayliss, Mark Millard, Lauren Seidman, and EEG reviewers Bill Haneberg, Skip Watts, and Neil Wells led to a number of improvements in the final text.

REFERENCES

Batschelet, E., 1981, *Circular Statistics in Biology*: Academic Press, London, 371 p.

Borradaile, G., 2003, *Statistics of Earth Science Data, Their Distribution in Time, Space, and Orientation*: Springer-Verlag, Berlin, 351 p.

Brunton Company, 2000, *Pocket Transit Instruction Manual*: The Brunton Company, Riverton, WY, 25 p.

Compton, R. R., 1962, *Manual of Field Geology*: John Wiley & Sons, New York, 378 p.

Fisher, N. I.; Lewis, T.; and Embleton, B. J. J., 1987, *Statistical Analysis of Spherical Data*: Cambridge University Press, Cambridge, United Kingdom, 329 p.

Fisher, R. A., 1953, Dispersion on a sphere: *Proceedings Royal Society, London*, Vol. A217, No. 1130, pp. 295–305.
Irving, E., 1964, *Paleomagnetism and its Application to Geological and Geophysical Problems*: John Wiley & Sons, New York, 399 p.
Mardia, K. V., 1972, *Statistics of Directional Data*: Academic Press, London, 357 p.
Opdyke, N. D. and Channell, J. E. T., 1996, *Magnetic Stratigraphy*: Academic Press, San Diego, CA, 346 p.
Tarling, D. H., 1971, *Principles and Applications of Palaeomagnetism*: Chapman and Hall, London, 164 p.
Tauxe, L., 1998, *Paleomagnetic Principles and Practices*: Kluwer Academic Publishers, Dordrecht, 299 p.